

Fig. 2. Doubler performance between 90 and 130 GHz when tuning and bias are optimized at each operating frequency. Constant pump power of 50 mW.

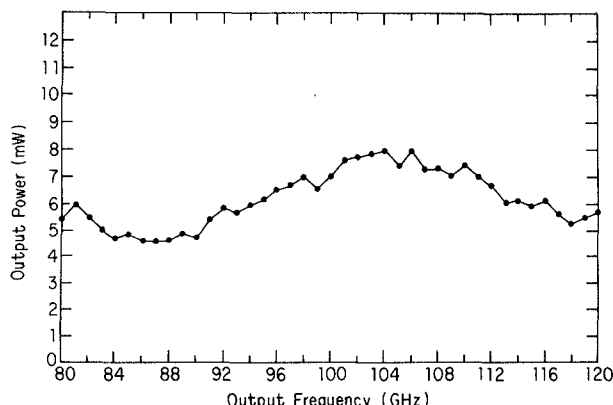


Fig. 3 Doubler performance between 80 and 120 GHz when tuning and bias are held fixed. Constant pump power of 50 mW.

low-pass filter. The line terminates on the center pin of the SMA bias connector. The section of bias line between capacitor and filter approximates, at 100 GHz, a quarter-wave short circuited stub of 140Ω characteristic impedance.

The varactor diodes used in these devices are notch front GaAs Schottky-barrier diodes supplied by the University of Virginia. The epilayer doping is $2.6 \times 10^{16} \text{ cm}^{-3}$ and the epilayer thickness is $1.5 \mu\text{m}$. The diode anode diameter is $5 \mu\text{m}$, resulting in a zero bias capacitance of 21 fF , a dc series resistance of 8Ω and a reverse breakdown voltage of 14.5 V . For reverse voltages of up to 12 V , the capacitance-versus-voltage law for these devices closely follows the inverse half-power law typical of abrupt junction varactors.

III. PERFORMANCE

When tuning and bias are optimized at each frequency, the output power response shown in Fig. 2, as a function of output frequency with constant pump power of 50 mW, is obtained. Minimum conversion efficiency is 18 percent for output frequencies between 90 and 124 GHz. Typically, the bias voltage for optimum performance is in the reverse direction and of about 4-V magnitude. The rapid decrease in efficiency above 124 GHz is due to the high frequency cutoff of the pump circuit stripline low-pass filter. The doubler is capable of operating continuously without performance degradation at pump powers less than or

equal to approximately 80 mW. Conversion efficiency changes by less than 1 percent at any frequency for pump powers greater than 40 mW, but below this power level the output power is approximately proportional to the square of the pump level.

The results shown in Fig. 3 were obtained with the doubler tuning fixed for both pump and output circuits. The dc bias supply was operated as a constant (3.0 mA) forward current sink. Under this condition, the reverse voltage applied to the diode varied between 2 and 6 V as the frequency was changed. Between 80- and 120-GHz output frequency with constant 50-mW pump power, the median conversion efficiency is 12 percent, with a total variation of less than 2.5 dB over this frequency range.

IV. CONCLUSION

An improved millimeter-wavelength frequency doubler has been described. The device exhibits good fixed-tuned broad-band performance, with a minimum output power of 4.2 mW, for 50-mW pump power, at any output frequency in the range 80 to 120 GHz. Maximum total variation in output power over this range is less than 2.5 dB when the pump power is held constant. The improvement in broad-band performance is attributed, firstly, to modifications made to the pump-frequency matching circuitry, with the addition of a series tuning stub and altered waveguide to stripline transition geometry. Secondly, empirical studies of the relationship between output waveguide impedance transformer dimensions and doubler performance gave rise to an improved transformer design which optimizes the effects of spurious mode coupling on broad-band conversion efficiency. Doublers similar to the unit described have operated reliably and continuously in operational receiver systems at the National Radio Astronomy Observatory for more than 10000 hours without failure.

ACKNOWLEDGMENT

The author gratefully acknowledges the able assistance of N. Horner, Jr. who assembled and tested the doubler mounts. Prof. R. Mattauch of the University of Virginia is thanked for providing the Schottky diodes used in these devices.

REFERENCES

[1] J. W. Archer, "Millimeter-wavelength frequency multipliers," *IEEE Trans. Microwave Theory Tech.*, vol. MTT-29, pp. 552-557, June 1981.

Spectral Domain Analysis of a Hexagonal Microstrip Resonator

ARVIND K. SHARMA, MEMBER, IEEE, and WOLFGANG J. R. HOEFER, SENIOR MEMBER, IEEE

Abstract—The capacitance of an open regular hexagonal microstrip resonator is calculated with the quasi-static spectral domain technique. From the capacitance values, the effective hexagon side and the effective dielectric constant are determined, yielding resonant frequencies which agree well with measured values. Numerical data for several dielectric

Manuscript received September 2, 1981; revised November 11, 1981. The authors are with the Department of Electrical Engineering, University of Ottawa, Ontario, K1N 6N5, Canada.

constants are included. The capacitance values are also compared with those of circular and triangular microstrip resonators. A simple formula relates the resonant frequencies of commensurate hexagonal and circular resonators.

I. INTRODUCTION

Microstrip resonant structures are network elements frequently employed in microwave integrated circuit design. Resonant structures of simple geometrical shapes such as rectangular, circular disk, and ring resonators have been used extensively in oscillators, filters, and circulators [1]–[3].

Resonant structures of various different geometrical shapes also find application in microwave networks, providing improved performance and better flexibility in the design. For instance, a stripline circulator using an apex-coupled equilateral triangular resonator [4] has a bandwidth three times as large as a circular disk [5]. Its insertion loss is also reported to be marginally better because its radiation Q -factor is higher than that of a circular disk [5].

For applications in harmonic multipliers and parametric amplifiers, elliptic disk resonators are preferred over circular disks because there exists a harmonic relationship among resonant modes of the elliptic microstrip disk resonator [7]–[9] when the eccentricity is appropriately chosen. Hence, there is considerable interest in the study of resonant structures of many different shapes [10]. One of these is the regular hexagonal microstrip resonator which has been used in the past as a junction resonator and as a circulator element [11].

This paper presents an analysis of a regular hexagonal microstrip resonator using the quasi-static formulation in the spectral domain. The effective hexagon side and the effective dielectric constant are calculated by determining the capacitance of the resonator with and without dielectric. These quantities are then utilized in the computation of the dominant resonant frequency. Measurements made on hexagonal resonators of various sizes of Epsilonum-10 ($\epsilon_r = 10.2$) and on RT-Duroid ($\epsilon_r = 2.22$) are in good agreement with the calculations.

II. METHOD OF ANALYSIS

Fig. 1 shows a regular hexagonal microstrip resonator with side a in an open configuration. The dielectric substrate of thickness d has a relative permittivity ϵ_r .

The quasi-static analysis of this structure is initiated by introducing the two-dimensional Fourier transform of the potential with respect to x - and z -axes, defined by

$$\tilde{\phi}(\alpha, y, \beta) = \int_{-\infty}^{\infty} \int_{-\infty}^{\infty} \phi(x, y, z) e^{j(\alpha x + \beta z)} dx dz \quad (1)$$

where the potential function $\phi(x, y, z)$ for a given charge density $\rho(x, z)$ on the structure satisfies Poisson's equation

$$\nabla^2 \phi(x, y, z) = -\frac{1}{\epsilon} \rho(x, z) \delta(y - d). \quad (2)$$

In order to satisfy the boundary conditions, the Fourier transforms of the charge density $\tilde{\rho}(\alpha, \beta)$ and potential $\tilde{\phi}(\alpha, d, \beta)$ are related by

$$\tilde{G}(\alpha, d, \beta) \tilde{\rho}(\alpha, \beta) = \tilde{\phi}(\alpha, d, \beta) \quad (3)$$

where $\tilde{G}(\alpha, d, \beta)$ is the Fourier transform of the Green's function

$$\tilde{G}(\alpha, d, \beta) = [\epsilon_0 \gamma (1 + \epsilon_r \coth \gamma d)]^{-1} \quad (4)$$

with

$$\gamma = (\alpha^2 + \beta^2)^{1/2}. \quad (5)$$

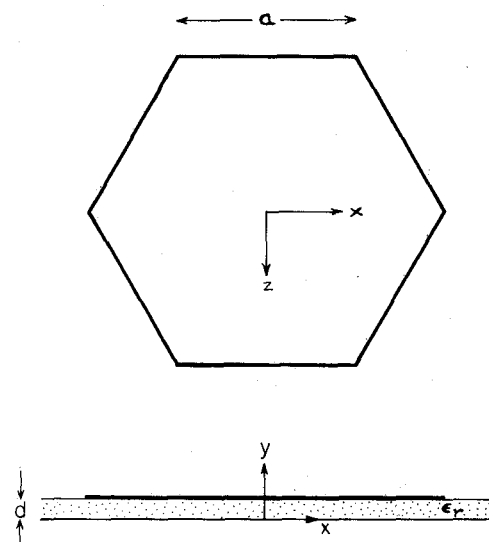


Fig. 1. Hexagonal microstrip resonator.

The Fourier transform of the potential $\tilde{\phi}(\alpha, d, \beta)$ is composed of $\tilde{\phi}_i(\alpha, d, \beta)$ which exists on the hexagon, and $\tilde{\phi}_0(\alpha, d, \beta)$ which exists on the region of the interface complementary to the hexagon. The unknown charge distribution on the structure is assumed to have the following form:

$$\rho(x, z) = \sum_{n=1}^N d_n \rho_n(x, z) \quad (6)$$

which in the Fourier transform domain becomes

$$\tilde{\rho}(\alpha, \beta) = \sum_{n=1}^N d_n \tilde{\rho}_n(\alpha, \beta) \quad (7)$$

where the unknown coefficients d_n must be determined. Since the charge density $\rho(x, z)$ and the potential $\phi_0(x, d, z)$ exist on the complementary regions of the interface, the unknown $\tilde{\phi}_0(\alpha, d, \beta)$ is eliminated through the application of Galerkin's procedure and Parseval's theorem. To that end, we define the following inner product:

$$\langle \tilde{\rho}_m(\alpha, \beta), \tilde{\rho}_n^*(\alpha, \beta) \rangle = \int_{-\infty}^{\infty} \int_{-\infty}^{\infty} \tilde{\rho}_m(\alpha, \beta) \tilde{\rho}_n^*(\alpha, \beta) d\alpha d\beta \quad (8)$$

where the superscript * denotes complex conjugate. Substituting (7) in (3), and taking the inner product of (3) with $\tilde{\rho}_m^*(\alpha, \beta)$ for $m = 1, 2, \dots, N$, yields the following algebraic equations:

$$\begin{aligned} \sum_{n=1}^N d_n \langle \tilde{G}(\alpha, d, \beta) \tilde{\rho}_n(\alpha, \beta), \tilde{\rho}_m^*(\alpha, \beta) \rangle \\ = \langle \tilde{\phi}_i(\alpha, d, \beta) + \tilde{\phi}_0(\alpha, d, \beta), \tilde{\rho}_m^*(\alpha, \beta) \rangle \end{aligned} \quad (9)$$

which upon application of Parseval's theorem reduces to

$$\begin{aligned} \sum_{n=1}^N d_n \langle \tilde{G}(\alpha, d, \beta) \tilde{\rho}_n(\alpha, \beta), \tilde{\rho}_m^*(\alpha, \beta) \rangle \\ = (2\pi)^2 \langle \phi_i(x, d, z), \rho_m(x, z) \rangle. \end{aligned} \quad (10)$$

The unknown constants d_n are evaluated using (10). The capaci-

tance C is then obtained from the expression

$$C = \sum_{n=1}^N d_n \int_S \int \rho_n(x, z) dx dz \quad (11)$$

where the region S is the surface bounded by lines

$$x = a \pm z/\sqrt{3} \quad (12a)$$

$$x = -a \pm z/\sqrt{3} \quad (12b)$$

$$z = \pm\sqrt{3}a/2. \quad (12c)$$

In the present analysis, we consider the following basis functions for the charge density function on the hexagon:

$$N=1: \quad \rho_1(x, z) = 1 \quad (13a)$$

$$N=2: \quad \rho_2(x, z) = \sqrt{x^2 + z^2} \quad (13b)$$

$$N=3: \quad \rho_3(x, z) = x^2 + z^2. \quad (13c)$$

The Fourier transform of the charge densities required in (10) and the integral over S in (11) can be easily calculated.

III. NUMERICAL AND EXPERIMENTAL RESULTS

Following the foregoing analysis, a computer program has been developed to evaluate the unknown coefficients d_n in the algebraic equations (10). The capacitance of the hexagon is then computed using (11) by assuming uniform charge density ($N=1$) as well as higher order charge density functions ($N=3$). The CPU time on an AMDAHL OS/VS1-0470 system is 10 s for $N=1$ while it is 110 s for $N=3$.

Fig. 2 presents the normalized capacitance C_N of the hexagonal resonator as a function of d/a . It is equal to C/C_0 , where C is the capacitance of the hexagon obtained using the present method, and C_0 is the parallel plate capacitance of the structure given by

$$C_0 = \epsilon_0 \epsilon_r \frac{3\sqrt{3}}{2} \frac{a^2}{d}. \quad (14)$$

For small values of d/a , the normalized capacitance tends toward unity. As d/a increases, C_N also increases. The capacitance variation is seen to be very similar to that of a circular microstrip disk [13]–[15].

The fringing associated with the regular hexagon structure can be assessed in terms of the normalized capacitance. The effective hexagon side \bar{a} is determined as

$$\frac{\bar{a}}{a} = \sqrt{C_N}. \quad (15)$$

The effective dielectric constant of the hexagonal resonator is determined as the ratio of the capacitance with the dielectric and without the dielectric

$$\epsilon_{\text{eff}}(d, a, \epsilon_r) = \frac{C(\epsilon = \epsilon_0 \epsilon_r)}{C(\epsilon = \epsilon_0)}. \quad (16)$$

The resonant frequency of the dominant mode is given by [16]

$$\frac{a}{\lambda_0} = \frac{2.011}{2\pi(\bar{a}/a)\sqrt{\epsilon_{\text{eff}}(d, a, \epsilon_r)}} \quad (17)$$

where λ_0 is the free-space wavelength. It is presented as a function of d/a in Fig. 3. Several hexagonal resonators have been realized on RT-Duroid ($\epsilon_r = 2.22$) and Epsilonum-10 ($\epsilon_r = 10.2$) substrates. The resonators were coupled to a 50- Ω microstrip line through a capacitive gap at the center of one hexagon side. The resonant frequency of hexagons on Epsilonum-10 substrate was measured in the transmission mode, and that of resonators on

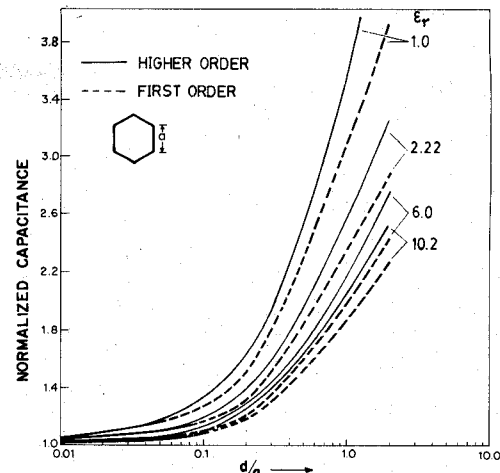


Fig. 2. Normalized capacitance of a hexagonal microstrip resonator as a function of d/a for several dielectric constants.

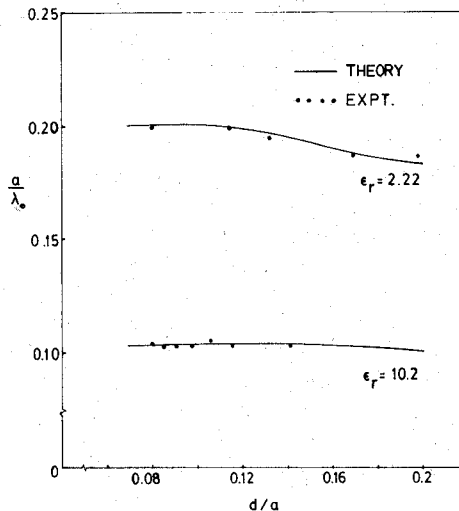


Fig. 3. Normalized resonant frequencies (a/λ_0) as a function of d/a for $\epsilon_r = 2.22$ and $\epsilon_r = 10.2$.

RT-Duroid in the reflection mode. In all cases, the influence of the coupling gap on the resonant frequency was negligible. In Fig. 3, the experimental values are shown against the background of numerically obtained values of the normalized resonant frequencies. Agreement is typically better than ± 2 percent for values of d/a less than 0.2.

IV. COMPARISON WITH THE EQUILATERAL TRIANGLE AND CIRCULAR DISK

A comparison of the static capacitance values $Cd/\epsilon_0 \epsilon_r a^2$ of the hexagonal, triangular, and circular disk resonators is provided in Fig. 4 for $\epsilon_r = 10.2$. The capacitance of the equilateral triangular resonator is taken from [10] which utilizes the present technique. The capacitance of the circular disk was obtained using the Hankel transform and Galerkin's procedure [13]–[15].

It was found that the resonant frequencies of the circular and hexagonal resonators of identical dimensions a are related by the following empirical expression:

$$\frac{f_{\text{hexagonal}}}{f_{\text{circle}}} = 1.05, \quad \text{for identical dimensions } a \quad (18)$$

provided that the ϵ_r is high ($\epsilon_r > 6$) and the ratio d/a less than unity.

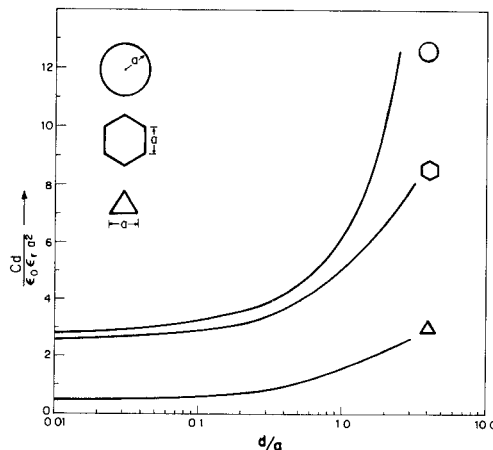


Fig. 4. Comparison of static capacitances of the hexagonal, the equilateral triangle, and the circular disk for $\epsilon_r = 10.2$

Since extensive data on the circular disk resonator are available in the literature, the resonant frequency of the commensurate hexagonal resonator can easily be computed from these data using (18). The error committed will be smaller than ± 2 percent.

V. CONCLUSION

This paper presents the analysis of hexagonal microstrip resonators under quasi-static approximations using the spectral domain technique. Theoretical results for their capacitance and resonant frequency are given for various dielectric constants. These values are compared with corresponding parameters of circular and triangular microstrip resonators. A simple empirical formula relates the resonant frequencies of hexagonal and circular resonators of identical dimensions. Experimental data on the hexagonal resonator agree within ± 2 percent with the computed results. Thus, the quasi-static formulation of the spectral domain technique can be utilized to predict fairly accurate resonant frequencies for the normalized hexagon side a/d less than 5.0.

REFERENCES

- [1] S. Mao, S. Jones, and G. D. Vendelin, "Millimeter-wave integrated circuits," *IEEE Trans. Microwave Theory Tech.*, vol. MTT-16, pp. 455-461, July 1968.
- [2] T. H. Oxley, "Microwave integrated circuit techniques," *Gen. Elec. Co. Ltd Engl. J. Sci. Technol.*, vol. 43, pp. 21-31, Jan. 1976.
- [3] G. D'Inzeo, F. Giannini, C. M. Sodi, and R. Sorrentino, "Method of analysis and filtering properties of microwave planar networks," *IEEE Trans. Microwave Theory Tech.*, vol. MTT-26, pp. 462-471, July 1978.
- [4] J. Helszajn and D. S. James, "Planar triangular resonators with magnetic walls," *IEEE Trans. Microwave Theory Tech.*, vol. MTT-26, pp. 95-100, Feb. 1978.
- [5] J. Helszajn, D. S. James, and W. T. Nisbet, "Circulators using planar triangular resonators," *IEEE Trans. Microwave Theory Tech.*, vol. MTT-26, pp. 188-193, Feb. 1979.
- [6] M. Cuhaci and D. S. James, "Radiation from triangular and circular resonators in microstrip," presented at 1977 IEEE MTT-S International Microwave Symp., (San Diego, CA), June 1977.
- [7] R. T. Irish, "Elliptic resonator and its use in microcircuit systems," *Electron. Lett.*, vol. 7, pp. 149-150, Apr. 1971.
- [8] J. G. Kretzschmar, "Theoretical results for the elliptic microstrip resonators," *IEEE Trans. Microwave Theory Tech.*, vol. MTT-20, pp. 342-343, May 1972.
- [9] A. K. Sharma and B. Bhat, "Spectral domain analysis of elliptic microstrip disk resonators," *IEEE Trans. Microwave Theory Tech.*, vol. MTT-28, pp. 573-576, June 1980.
- [10] A. K. Sharma, "Spectral domain analysis of microstrip resonant structures," Ph.D. dissertation, Indian Institute of Technology, Delhi, Dec. 1979.
- [11] W. T. Nisbet and J. Helszajn, "Mode chart for microstrip resonators on dielectric and magnetic substrates using a transverse resonance method," *Microwaves, Opt. Acoust.*, vol. 3, pp. 69-77, March 1979.
- [12] Y. Rahmat-Samii, T. Itoh, and R. Mittra, "A spectral domain analysis

for solving microstrip discontinuity problems," *IEEE Trans. Microwave Theory Tech.*, vol. MTT-22, pp. 372-378, Apr. 1974.

- [13] T. Itoh and R. Mittra, "A new method for calculating the capacitance of circular disk for microwave integrated circuits," *IEEE Trans. Microwave Theory Tech.*, vol. MTT-21, pp. 431-432, June 1973.
- [14] T. Itoh and R. Mittra, "Analysis of microstrip disk resonators," *Arch. Elek. Übertragung*, vol. 27, pp. 456-458, Nov. 1973.
- [15] A. K. Sharma and B. Bhat, "Influence of shielding on the capacitance of shielded microstrip disk and ring structures," *Arch. Elek. Übertragung*, vol. 34, pp. 41-44, Jan. 1980.
- [16] J.-P. Hsu, O. Kondo, T. Anada, and H. Makino, "Measurement and calculation of eigenvalues of various triplate-type microwave planar circuits," *Rec. Prof. Groups, IECEJ*, paper MW 73-117, Feb. 23, 1974.

S-Parameter Equivalents of Current and Voltage Noise Sources in Microwave Devices

A. D. SUTHERLAND, SENIOR MEMBER, IEEE, AND
M. W. TRIPPE

Abstract — The representation of noise sources in terms of signal flow graph equivalents is derived, enabling one to model noisy electron devices in terms of their *S*-parameters.¹

I. INTRODUCTION

The characterization of the noise of electron devices at low and moderate frequencies invariably involves the introduction of series noise voltage sources or shunt noise current sources embedded in a network of impedances or admittances which includes additional controlled current or voltage sources to model the nonreciprocal behavior of the device. For example, the equivalent circuit devised by van der Ziel [1] for field-effect transistors in a common source configuration (Fig. 1) contains two noise current sources shunting the input (gate-source) and output (drain-source) terminals of that device (i.e., i_g and i_d).

Microwave devices are most conveniently characterized in terms of their scattering matrix elements (*S*-parameters). Not only are those parameters readily measured but, also, through the use of signal flow graphs, they provide a very convenient means for analysis when such devices are embedded between input and output networks which serve the purposes of providing dc bias voltages or currents, and acting as impedance transformers. It is the purpose of this short paper to demonstrate how one can also represent the presence of the noise current or voltage sources of the device in such signal flow graphs. This can be used for the purpose of analyzing the noise performance of the device in its embedding environment or, conversely, for the purpose of deducing from noise measurements the values of those equivalent *S*-parameter noise sources.

We adopt the convention prevalent in noise literature of using lower case symbols (e , i , v , etc.) to represent rms noise phasors. Because they are randomly time-dependent, they are char-

Manuscript received October 12, 1981; revised December 15, 1981. This work was supported by the National Science Foundation under Grant ENG-78-00797.

The authors are with the Department of Electrical Engineering, University of Florida, Gainesville, FL 32611.

¹The research leading to the results described herein was suggested by A. van der Ziel.